Inorg. Chem. **2006**, *45*, 6816–6827

^{13}C and ^{15}N NMR Studies of Iron-Bound Cyanides of Heme Proteins and Related Model Complexes: Sensitive Probe for Detecting Hydrogen-bonding Interactions at the Proximal and Distal Sides

Hiroshi Fujii*,† and Tadashi Yoshida‡

Institute for Molecular Science and Okazaki Institute for Integrative Bioscience, National Institutes of Natural Sciences, Myodaiji, Okazaki 444-8787, Japan, and Yamagata University School of Medicine, Yamagata 990-9585, Japan

Received May 1, 2006

Studies of the ^{13}C and ^{15}N NMR paramagnetic shifts of the iron-bound cyanides in the ferric cyanide forms of various heme proteins containing the proximal histidine and related model complexes are reported. The paramagnetic shifts of the ^{13}C and ^{15}N NMR signals of the iron-bound cyanide are not significantly affected by the substitution of the porphyrin side chains. On the other hand, the paramagnetic shifts of both the ^{13}C and ^{15}N NMR signals decrease with an increase in the donor effect of the proximal ligand, and the ^{13}C NMR signal is more sensitive to a modification of the donor effect of the proximal ligand than the ^{15}N NMR signal. With the tilt of the iron–imidazole bond, the paramagnetic shift of the ^{13}C NMR signal increases, whereas that of the ^{15}N NMR signal decreases. The hydrogen-bonding interaction of the iron-bound cyanide with a solvent decreases the paramagnetic shift of both ^{13}C and ^{15}N NMR signals, and the effect is more pronounced for the ^{15}N NMR signal. Data on the ^{13}C and ^{15}N NMR signals of iron-bound cyanide for various heme proteins are also reported and analyzed in detail. Substantial differences in the ^{13}C and ^{15}N NMR shifts for the heme proteins can be explained on the basis of the results for the model complexes and structures around the heme in the heme proteins. The findings herein show that the paramagnetic shift of the ^{13}C NMR signal of the iron-bound cyanide is a good probe to estimate the donor effect of the proximal imidazole and that the ratio of $^{15}N/^{13}C$ NMR shifts allows the hydrogen-bonding interaction on the distal side to be estimated.

Introduction

There has been intense interest in developing a better understanding of structure−function relationships in heme proteins for many years. The primary control of the function of heme proteins is generally thought to involve both steric and electronic influences by the proximal ligand and amino acid residues near the active site.[1−4] The amino acids around the heme in a heme protein are important determinants of the function of the protein. For example, in myoglobin, the electron-donor effect exerted by the proximal histidine and hydrogen-bonding interactions involving the distal histidine are essential for its function: stabilizing the iron bound oxygen.[5−8] Therefore, characterization of the protein machinery becomes a crucial issue in understanding the function of heme proteins, and facile and sensitive spectroscopic probes for evaluating the protein machinery, using various spectroscopic methods, have been developed.

The heme iron in a heme protein can bind various types of small molecules.[5,9] Some of these small molecules, especially those that form stable complexes, have been used

* To whom correspondence should be addressed. E-mail: hiro@ims.ac.jp. Phone: +81-564-59-5578. Fax: +81−564−59−5600.
† Institute for Molecular Science and Okazaki Institute for Integrative Bioscience.
‡ Yamagata University.

(1) Poulos, T. M. *Adv. Inorg. Biochem.* **1988**, *7*, 1−36.
(2) James, B. R. In *The Porphyrins*; Dolphin, D. Ed.; Academic Press: New York, 1978; Vol. V, pp 205−302.
(3) Dawson, J. H.; Sono, M. *Chem. Rev.* **1987**, *87*, 1255−1275.
(4) Peisach, J.; Blumberg, W. E.; Alder, A. *Ann. N. Y. Acad. Sci.* **1973**, *206*, 310−326.
(5) Springer, B. A.; Sligar, S. G.; Olson, J. S.; Phillips, G. N., Jr. *Chem. Rev.* **1994**, *94*, 699−714.
(6) Adachi, S.; Nagano, S.; Ishimori, K.; Watanabe, Y.; Morishima, I.; Egawa, T.; Kitagawa, T.; Makino, R. *Biochemistry* **1993**, *32*, 241−252.
(7) Egeberg, K. D.; Springer, B. A.; Martinis, S. A.; Sligar, S. G.; Morikis, D.; Champion, P. M. *Biochemistry* **1990**, *29*, 9783−9791.
(8) Depillis, G. D.; Decatur, S. M.; Barrick, D.; Boxer, S. G. *J. Am. Chem. Soc.* **1994**, *116*, 6981−6982.

10.1021/ic0607383 CCC: $33.50
Published on Web 07/25/2006

as spectroscopic probes in various spectroscopic methods.[10] In multinuclear NMR spectroscopies, these small iron-bound molecules have great potential for serving as useful NMR probes for characterization of the environment and electronic structure of prosthetic groups in heme proteins.[11] In this regard, the diamagnetic ferrous states have been thoroughly examined because of the ease of signal detection of a small molecule bound to iron. The ^{13}C NMR signals of ^{13}CO and isocyanides, R−N^{13}C, bound to heme proteins were found to be sensitive to the nature of the trans amino acid ligand.[12−14] The ^{13}C NMR signals of heme bound ^{13}CO can be used to differentiate between the heme moieties of the α and β subunits of hemoglobin, but these ^{13}C shifts were not sensitive to variations in the species from which the hemoglobins are derived and to pH variations, possibly because these ^{13}C NMR shifts are diamagnetic in origin.[12] ^{17}O NMR spectra of heme-bound C^{17}O and $^{17}O_2$ have also been used for studying the binding structures of CO and O_2 in heme proteins.[14−16]

For the paramagnetic ferric state, the cyanide ion would appear to have the greatest potential because of its extremely high affinity for the ferric heme iron center.[11] ^{13}C and ^{15}N NMR spectroscopies for iron-bound cyanide would be expected to be very sensitive probes because the ferric paramagnetic iron center amplifies small structural and electronic changes that occur around the heme and allows them to be easily detected by their NMR shifts. The ^{15}N NMR signals of the iron-bound C^{15}N were located in the far-downfield region for both the iron(III) porphyrin model complexes and the heme proteins, and the ^{15}N NMR signals of the iron-bound cyanide have been used to study the protein machinery of various heme proteins.[17−19] However, it was difficult to distinguish the electron-donor effect of the proximal ligand from the hydrogen-bonding effect of the distal amino acids using ^{15}N NMR spectroscopy because the ^{15}N NMR shift reflects both effects.[17,18] Thus, ^{15}N NMR spectroscopy remains ambiguous as an NMR probe. On the other hand, ^{13}C NMR spectroscopy of iron-bound ^{13}CN has been investigated in less detail.[20−22] The ^{13}C NMR signals of the iron-bound ^{13}CN of the biscyanide iron(III) porphyrin model complexes were located in the far-upfield region (∼−2500 ppm from TMS), but the extreme line-broadening of the signal appeared to preclude signal detection in the heme proteins.[20] We recently succeeded in the first detection of ^{13}C NMR signals of an iron-bound ^{13}CN in ferric cyanide complexes of heme proteins in an unexpectedly large upfield region (∼−4000 ppm from TMS).[21] The ^{13}C NMR signals of the iron-bound cyanides of some heme proteins showed different NMR shifts, which are presumed to be related to the nature of the proximal ligand.

Here, we report on a comprehensive study of the ^{13}C and ^{15}N NMR spectra of the iron-bound cyanide of various ferric heme proteins with a proximal histidine and some related model complexes. To analyze the factors that influence the ^{13}C and ^{15}N NMR shifts in heme proteins, we study effects of the porphyrin, the proximal ligand, and solvent on the iron-bound ^{13}C and ^{15}N NMR shifts of heme protein model complexes. The ^{13}C NMR shift of the iron-bound cyanide mainly reflects the donor effect of the proximal imidazole, while the ^{15}N NMR shift of the iron-bound cyanide reflects both the donor effect of the proximal imidazole and the hydrogen-bonding interaction from a solvent. Substantial differences in the ^{13}C and ^{15}N NMR shifts for various heme proteins can be explained on the basis of the NMR results obtained for model complexes and the active site structures of the heme proteins. The findings herein demonstrate that the ^{13}C NMR signal of the iron-bound cyanide is a good probe with which to estimate the donor effect of the proximal imidazole and that the ratio of the ^{15}N/^{13}C NMR shifts allows the hydrogen-bonding interaction on the distal side to be estimated.

Experimental Section

Abbreviations. The following abbreviations were used throughout this paper: CN, cyanide; ImH, imidazole; 1-Me-Im, 1-methylimidazole; 1-Ph-Im, 1-phenylimidazole; 1-Ac-Im, 1-acetylimidazole; Im$^-$, imidazolate; Py, pyridine; DMAP, 4-(dimethylamino)pyridine; 4-Me-Py, 4-methylpyridine; 4-Ac−Py, 4-acetylpyridine; 4-CN-Py, 4-cyanopyridine; PPDME, protoporphyrinIX dimethylester; MPDME, mesoporphyrinIX dimethylester; DPDME, deuteroporphyrinIX dimethylester; DAPDME, 2,4-diacetyldeuteroporphyrin dimethylester; PP, protoporphyrinIX; TMS, tetramethylsilane; DMSO, dimethyl sulfoxide; ENDOR, electron−nuclear double resonance; Mb, myoglobin; Hb, hemoglobin; Cyt c, cytochrome *c*; HRP, horseradish peroxidase; ARP, *Arthromyces ramosus* peroxidase; HO, heme oxygenase; PigA-HO, heme oxygenase of *Pseudomonas aeruginosa*.

(9) Antonini, E.; Brunori, M. *Hemoglobin and Myoglobin in Their Reactions with Ligands*; Elsevier Science Publishers B. V.: Amsterdam, 1971.

(10) Spiro, T. G.; Wasbotten, I. H. *J. Inorg. Biochem.* **1999**, *205*, 34−44.

(11) (a) Walker, F. A. In *The Porphyrin Handbook*; Kaddish, K. M., Smith, K. M., Guilard, R., Eds.; Academic Press: San Diego, CA.; 2000; Vol. 5, pp 81−183. (b) Goff, H. M. In *Iron Porphyrins*; Lever, A. B. P., Gray, H. B., Eds.; Addison-Wesley: Reading, MA, 1983; Part 1, pp 237−281. (c) La Mar, G. N.; Walker, F. A. In *The Porphyrins*; Dolphin, D. Ed.; Academic Press: New York, 1978; Vol. IV, pp 61−157.

(12) (a) Moon, R. B.; Richards, J. H. *J. Am. Chem. Soc.* **1972**, *94*, 5093−5095. (b) Moon, R. B.; Richards, J. H. *Biochemistry* **1974**, *13*, 3437−3443. (c) Moon, R. B.; Dill, K.; Richards, J. H. *Biochemistry* **1977**, *16*, 221−228.

(13) Mansuy, D.; Lallemand, J.-Y.; Chottard, J.-C.; Cendried, B.; Gacon, G.; Wajcman, H. *Biochem. Biophys. Res. Commun.* **1976**, *70*, 595−599.

(14) McMahon, M. T.; deDios, A. C.; Godbout, N.; Salzmann, R.; Laws, D.; Le, H.; Havlin, R. H.; Oldfield, E. *J. Am. Chem. Soc.* **1998**, *120*, 4784−4797.

(15) (a) Park, K. D.; Guo, K.; Adebodun, F.; Chiu, M. L.; Sligar, S. G.; Oldfield, E. *Biochemistry* **1991**, *30*, 2333−2347. (b) Oldfield, E.; Lee, H. C.; Coretsopoulos, C.; Adebodun, F.; Park, K. D.; Yang, S.; Chung, J.; Phillips, B. *J. Am. Chem. Soc.* **1991**, *113*, 8680−8685.

(16) (a) Gerothanassis, I. P.; Momenteau, M. *J. Am. Chem. Soc.* **1987**, *109*, 6944−6947. (b) Gerothanassis, I. P.; Momenteau, M.; Loock, B. *J. Am. Chem. Soc.* **1989**, *111*, 7006−7012.

(17) (a) Morishima, I.; Inubushi, T. *J. Am. Chem. Soc.* **1978**, *100*, 3568−3574. (b) Shiro, Y.; Iizuka, T.; Makino, R.; Ishimura, Y.; Morishima, I. *J. Am. Chem. Soc.* **1989**, *111*, 7707−7711.

(18) (a) Behere, D. V.; Gonzalez-Vergara, E.; Goff, H. M. *Biochim. Biophys. Acta* **1985**, *832*, 319−325. (b) Behere, D. V.; Ales, D. C.; Goff, H. M. *Biochim. Biophys. Acta* **1986**, *871*, 285−292.

(19) Banci, L.; Bertini, I.; Kuan, I.-C.; Tien, M.; Turano, P.; Vila, A. J. *Biochemistry* **1993**, *32*, 13483−13489.

(20) Goff, H. M. *J. Am. Chem. Soc.* **1977**, *99*, 7723−7725.

(21) Fujii, H. *J. Am. Chem. Soc.* **2002**, *124*, 5936−5937.

(22) (a) Mao, J.; Oldfield, E. *J. Am. Chem. Soc.* **2002**, *124*, 13911−13920. (b) Hada, M. *J. Am. Chem. Soc.* **2004**, *126*, 486-487.

Materials. ProtoporphyrinIX dimethyl ester (PPDME) was prepared by a previously published method.[23] DeuteroporphyrinIX dimethyl ester (DPDME), mesoporphyrinIX dimethyl ester (MPDME), and 2,4-diactyldeuteroporphyrinIX dimethyl esters (DAPDME) were purchased from Aldrich. The incorporation of iron into the porphyrins was performed in acetic acid with ferrous chloride and sodium acetate.[23] All iron porphyrin complexes were purified by silica gel column chromatography. Hemin, chloro iron(III) protoporphyrinIX (PP), was purchased from Sigma and was used without further purification. Myoglobin from horse heart (horse-Mb), cytochrome *c* from horse heart (horse-Cyt c), cytochrome *c* from *Saccharomyces cerevisiae* (yeast-Cyt c), and cytochrome *c* from bovine heart (bovine-Cyt c) were purchased from Sigma and were used without further purification. Sperm whale myoglobin (whale-Mb) and horseradish peroxidase (HRP), RZ > 3.0, were obtained from Funakoshi (Tokyo, Japan) and were used without further purification. *A. ramosus* peroxidase (ARP), RZ > 2.5, was purchased from Nacalai Tesque (Kyoto, Japan) and was also used without further purification. An alanine mutant of the distal hisitidine in whale-Mb (H64A) was expressed in *Escherichia coli* and purified by previously published methods.[24] Rat heme oxygenase-1 (rat-HO-1), its alanine mutant of glutamate-29 (rat-HO-1 E29A), and the heme oxygenase of *Pseudomonas aeruginosa* (PigA-HO) were expressed in *E. coli* and purified by previously published method.[25] $K^{13}C^{15}N$ (99% enrichment) was purchased from ISOTEC Inc. (Miamisburg, OH). All other chemicals were purchased from commercial sources.

Measurements. Cyanide−imidazole complexes of iron(III) porphyrins were prepared by the addition of 1 equiv of $K^{13}C^{15}N$ in DMSO-d_6 and 1 equiv of the imidazole in CD_2Cl_2.[26] The cyanide−imidazolate complex was prepared by deprotonation of the imidazole NH proton of a cyanide imidazole complex by treatment with 1.2 equiv of sodium hydroxide solution in CD_3OD.[27] The ferric heme proteins were dissolved in 0.1 M phosphate buffer in D_2O, pH(D) = 7.0. The ferric cyanide complexes of heme proteins were prepared by the addition of excess $K^{13}C^{15}N$. The pH(D) of the NMR samples were monitored using a Horiba F-22 pH meter and the values are listed in Table 2. EPR spectra were recorded on Bruker E500 X-band spectrometer with an Oxford Instruments ESR910 helium-flow cryostat. ^{13}C and ^{15}N NMR spectra of the model complexes and heme proteins were obtained on JEOL Lambda-500 spectrometer. ^{13}C NMR spectra were typically obtained at sweep-widths of 200 kHz at 125.27 MHz with using 4 K data points. ^{15}N NMR spectra were obtained at sweep-widths of 100 kHz at 50.73 MHz with using 4 K data points. The pulse repetition time and pulse width were 0.075 s and 8 μs, respectively. Typically, 100 000 transients were collected for the model complexes, and 1 000 000 transients were collected for the heme proteins. The sample concentrations of the model complexes and heme proteins were ~10 and ~3 mM, respectively. The chemical shift values of the ^{13}C and ^{15}N NMR spectra are referenced to external tetramethylsilane (TMS) in chloroform and sodium nitrate ($^{15}NO_3^-$) in deuterium oxide, respectively.

Analysis of Paramagnetic Shifts of ^{13}C and ^{15}N NMR Signals. The ^{13}C and ^{15}N NMR data were analyzed by the following method. The observed NMR paramagnetic shifts of the iron-bound cyanides are the sum of the diamagnetic shift that is the NMR shift of the original cyanide ion and the isotropic paramagnetic shift that is the NMR shift induced by the paramagnetic ferric heme iron center, as shown in eq 1.[11,28] The diamagnetic shifts of the ^{13}C and ^{15}N

$$\left(\frac{\Delta H}{H}\right)^{\mathrm{par}} = \left(\frac{\Delta H}{H}\right)^{\mathrm{iso}} + \left(\frac{\Delta H}{H}\right)^{\mathrm{dia}} \quad (1)$$

NMR signals of iron-bound cyanide could be estimated from the ^{13}C and ^{15}N NMR shifts of a diamagnetic compound such as potassium ferrocyanide, $K_4Fe(CN)_6$; ^{13}C, +177 ppm from TMS; ^{15}N, −111 ppm from $^{15}NO_3^-$.[20,29] The isotropic paramagnetic shift consists of a dipolar shift resulting from a through-space dipolar interaction between the ^{13}C or ^{15}N atom of cyanide and the ferric heme iron center and a contact shift resulting from the delocalization of electron spin into an orbital on the ^{13}C or ^{15}N atom, as shown eq 2.[11,28] Since the dipolar shift can be roughly estimated from the

$$\left(\frac{\Delta H}{H}\right)^{\mathrm{iso}} = \left(\frac{\Delta H}{H}\right)^{\mathrm{con}} + \left(\frac{\Delta H}{H}\right)^{\mathrm{dip}} \quad (2)$$

EPR g parameters and the distance between the heme iron and the C or N atom of the iron bound-cyanide, as shown in eq 3,[11,28] we

$$\left(\frac{\Delta H}{H}\right)^{\mathrm{dip}} = \frac{\beta^2 S(S+1)}{9kT}\left(g_1{}^2 - \frac{g_2{}^2 + g_3{}^2}{2}\right)\left\langle\frac{3\cos^2\theta - 1}{r^3}\right\rangle \quad (3)$$

calculated the ^{13}C and ^{15}N contact and dipolar shifts of the iron-bound cyanides of the ferric heme proteins and their model complexes.[30−33] From the ^{13}C and ^{15}N contact shifts, we further calculated the isotropic hyperfine-coupling constants, A_{iso}, of the ^{13}C and ^{15}N atoms of the iron-bound cyanide, according to eq 4.[11,28]

$$\left(\frac{\Delta H}{H}\right)^{\mathrm{con}} = A_{\mathrm{iso}}\frac{|\gamma_{\mathrm{e}}|}{|\gamma_{\mathrm{N}}|}\frac{S(S+1)}{3kT} \quad (4)$$

where β is the Bohr magneton, g_1, g_2, and g_3 are the EPR g parameters, θ is the angle between the nucleus−metal vector and the z axis, r is the length of this vector, k is the Boltzman constant, T is the temperature used in the NMR measurement, A is an isotropic hyperfine coupling constant, S is the electron spin, $S = 1/2$, and γ_{N} and γ_{e} are the magnetogyric ratios of a nuclei and an electron.

Results

^{13}C and ^{15}N NMR Spectra for Heme Protein Model Complexes. To study the electronic effect of porphyrin on the ^{13}C and ^{15}N NMR shifts of the iron-bound cyanide, ^{13}C and ^{15}N NMR spectra were obtained for cyanide-1-methylimidzaole complexes of iron(III) PPDME, MPDME, DP-

(23) Fuhrhop, J.-H. In *Porphyrins and Mtealloporphyrins*; Smith, K. M., Ed.; Elsevier: Amsterdam, 1975; pp 757−869.
(24) Springer, B. A.; Egeberg, K. D.; Sligar, S. G.; Rohlfs, R. J.; Mathews, A. J.; Olson, J. S. *J. Biol. Chem.* **1989**, *264*, 3057−3060.
(25) (a) Takahashi, S.; Wang, J.; Rousseau, D. L.; Ishikawa, K.; Yoshida, T.; Host, J. R.; Ikeda-Saito, M. *J. Biol. Chem.* **1994**, *269*, 1010−1014. (b) Ito-Maki, M.; Ishikawa, K.; Matera, K. M.; Sato, M.; Ikeda-Saito, M.; Yoshida, T. *Arch. Biochem. Biophys.* **1995**, *317*, 253−258. (c) Fujii, H.; Zhang, X.; Yoshida, T. *J. Am. Chem. Soc.* **2004**, *126*, 4466−4467.
(26) La Mar, G. N.; Del Gaudio, J.; Frye, J. S. *Biochim. Biophs. Acta* **1979**, *498*, 422−435.
(27) (a) Chacko, V. P.; La Mar, G. N. *J. Am. Chem. Soc.* **1982**, *104*, 7002−7007. (b) Quinn, R.; Nappa, M.; Valentine, J. S. *J. Am. Chem. Soc.* **1982**, *104*, 2588−2595.
(28) (a) Jesson, J. P. In *NMR of Paramagnetic Molecules*; La Mar, G. N., Horrocks, W. D., Jr., Holm, R. H., Eds.; Academic Press: New York, 1973; pp 1−52. (b) Ming, L.-J. In *Physical Methods in Bioinorganic Chemistry*; Que, L., Jr., Ed.; University Science Book: Sausalito, CA, 2000; pp 375−464.
(29) Herbinson-Evans, D.; Richards, R. E. *Mol. Phys.* **1964**, *8*, 19−31.
(30) Hori, H. *Biochim. Biophys. Acta* **1971**, *251*, 227−235.
(31) Shulman, R. G.; Glarum, S. H.; Karplus, M. *J. Mol. Biol.* **1971**, *57*, 93−115.
(32) Brautigan, D.; Feinberg, B. A.; Hoffman, B. M.; Margolish, E.; Peisach, J.; Blumberg, W. E. *J. Biol. Chem.* **1977**, *252*, 574−582.
(33) Morita, Y.; Mason, H. S. *J. Biol. Chem.* **1965**, *240*, 2654−2659.

Scheme 1

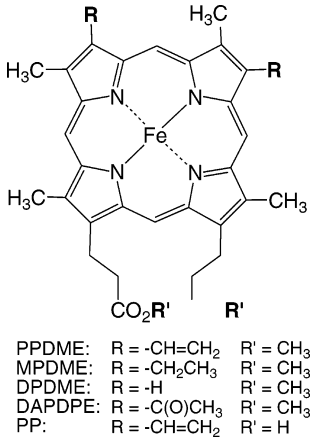

DME, and DAPDME in CD_2Cl_2 at 298 K (Scheme 1 and Figure 1). For all complexes, the ^{13}C NMR signals of the iron-bound cyanide are in an extremely upfield region around −4000 ppm from TMS, while the ^{15}N NMR signals of the iron bound cyanide are located in the far upfield region around +1000 ppm from $^{15}NO_3^-$. The ^{13}C and ^{15}N NMR signals shift slightly upfield with an increase in the electron-donating effect of a substituent at the 2,4-position. The electronic effect of the substituents at the 2,4-positions of porphyrin is known to alter its physical properties;[35] however, a drastic change was not seen in either the ^{13}C or ^{15}N NMR shifts of the iron-bound cyanide of iron(III) porphyrins containing various 2,4-substituents. A similar result was obtained when imidazole was used as an axial ligand instead of 1-methylimidazole (Table 1). We also obtained ^{13}C and ^{15}N NMR spectra of the iron-bound cyanide for hemin, iron-(III) PP, to examine the effect of a carboxylic acid moiety of the heme propionate, in terms of NMR shifts. The ^{13}C and ^{15}N NMR signals of the iron-bound cyanide of hemin are located at −4001 and 1010 ppm for the 1-methylimidazole complex and −3967 and 1010 ppm for the imidazole

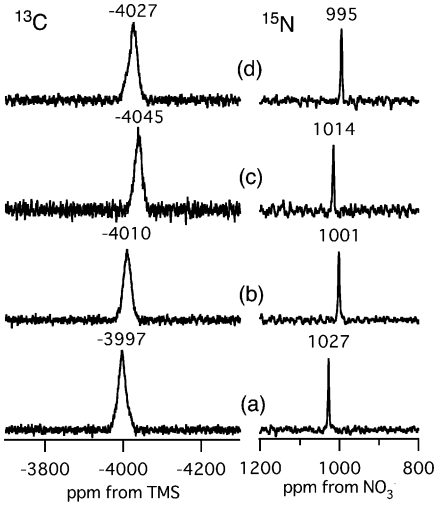

Figure 1. ^{13}C (left) and ^{15}N (right) NMR spectra of cyanide-1-methylimidazole complexes of various iron(III) various porphyrins in CD_2Cl_2 at 298 K: (a) DAPDMP, (b) PPDME, (c) DPDME, and (d) MPDME.

complex, respectively (Table 1). These ^{13}C and ^{15}N NMR shifts for iron(III) PP are very close to those for iron(III) PPDME. Therefore, the carboxylic acid moiety of the heme propionate has a negligible effect on the ^{13}C and ^{15}N NMR shifts of iron-bound cyanide. Collectively, these results indicate that the ^{13}C and ^{15}N NMR shifts of the iron-bound cyanide are not significantly affected by the nature of the porphyrin substituents.

We also examined the electronic effect of the axial ligand on the ^{13}C and ^{15}N NMR shifts of iron-bound cyanide. Figure 2 shows ^{13}C and ^{15}N NMR spectra of the iron-bound cyanide of iron(III) PPDME with a different pyridine as an axial ligand, $(PPDME)Fe^{III}(^{13}C^{15}N)(L)$, in CD_2Cl_2 at 298 K. The resonance positions of the ^{13}C and ^{15}N NMR signals of the iron-bound cyanides were moved to downfield and upfield, respectively, with an increase in the pK_a value of pyridine

Table 1. ^{13}C and ^{15}N NMR Chemical Shifts of Iron-Bound Cyanide for Iron(III) Porphyrin Complexes at 298 K

iron porphyrin	axial ligand	solvent	^{13}C NMR shift	^{15}N NMR shift
PPDME	1-methylimidazole	CD_2Cl_2	−4010	1001
	1-methylimidazole	DMSO-d_6	−4004	1012
	1-phenylimidazole	CD_2Cl_2	−4066	1026
	1-acetylimidazole	CD_2Cl_2	−4139	998
	1,2-dimethylimidazole	CD_2Cl_2	−4148	918
	1-methylimidazole	CD_2Cl_2−CD_3OD (22%)	−3952	866
	imidazole	CD_2Cl_2	−3926	1015
	imidazolate	CD_2Cl_2	−3507	733 (738[a])
DADPDME	1-methylimidazole	CD_2Cl_2	−3997	1027
	imidazole	CD_2Cl_2	−3905	
MPDME	1-methylimidazole	CD_2Cl_2	−4027	995
	imidazole	CD_2Cl_2	−3928	
DPDME	1-methylimidazole	CD_2Cl_2	−4045	1014
	imidazole	CD_2Cl_2	−3940	
PP	imidazole	DMSO-d_6	−3967	1010
	1-methylimidazole	DMSO-d_6	−4001	1010
	1-methylimidazole	DMDO-d_6−H_2O (30%)	−3934	904
	1-methylimidazole	DMSO-d_6−H_2O (50%)	−3875	830
	4-(dimethylamino)pyridine	DMSO-d_6	−3968	984
	4-methylpyridine	DMSO-d_6	−4121	1055
	pyridine	DMSO-d_6	−4158	1058
	4-acetylpyridine	DMSO-d_6	−4195	1055
	4-cyanopyridine	DMSO-d_6	−4269	1152

[a] Ref 18a.

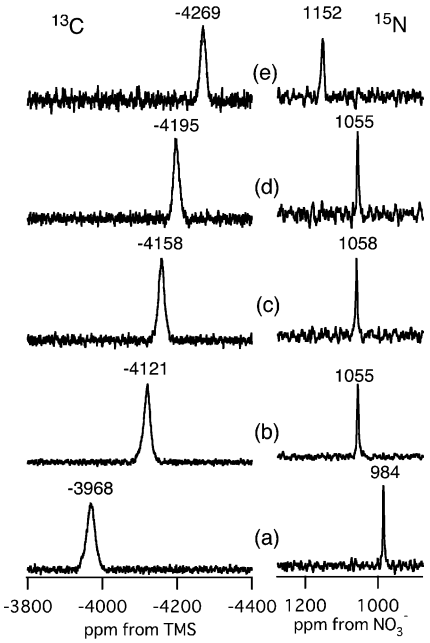

Figure 2. ^{13}C (left) and ^{15}N (right) NMR spectra of cyanide complexes of iron(III) protoporphyrinIX with various pyridines as axial ligands in DMSO-d_6 at 298 K: (a) 4-(dimethylamino)pyridine, (b) 4-methylpyridine, (c) pyridine, (d) 4-acetylpyridine, and (e) 4-cyanopyridine.

(going from Figure 2e to a).[36] This indicates that the ^{13}C and ^{15}N paramagnetic shifts of iron-bound cyanide decrease with an increase in the donor effect of the axial ligand. The trans effect induced by the change in the axial ligand is much more pronounced than the cis effect, which is caused by the substitution of the peripheral groups on porphyrin. A similar result was obtained for the ^{13}C NMR signal when various imidazole derivatives were used as axial ligands (Figure S1 and Table 1). However, significant change was not found for the ^{15}N NMR signal because the pK_a range (3.6−7.2) of the imidazole derivatives was narrower than that (1.9−9.7) for the pyridine derivatives.[36] These results clearly show that the ^{13}C and ^{15}N NMR shifts of the iron-bound cyanide decrease with an increase in the donor effect of the proximal ligand, and the ^{13}C NMR signal is more sensitive to a modification of the donor effect of the proximal ligand than the ^{15}N NMR signal.

To investigate the steric effect of the axial imdazole on ^{13}C and ^{15}N NMR shifts, we obtained ^{13}C and ^{15}N NMR spectra of the cyanide complex of iron(III) PPDME with 1,2-dimethylimidazole as an axial ligand (Figure 3). A substituent at the 2-position of imidazole induces steric repulsion with the porphyrin plane, resulting in a tilt in the iron−imidazole bond.[37] The ^{13}C and ^{15}N NMR signals of the iron-bound cyanide of the 1,2-dimethylimidazole complex of iron(III)

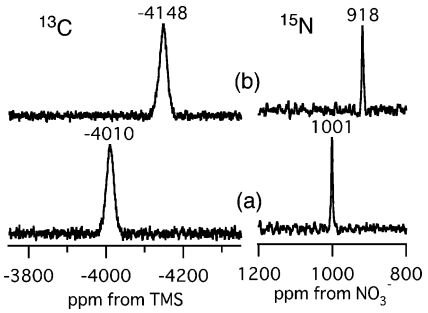

Figure 3. ^{13}C (left) and ^{15}N (right) NMR spectra of cyanide complexes of iron(III) PPDME with various imidazole axial ligands at 298 K: (a) 1-methylimidazole complex and (b) 1,2-dimethylimidazole complex.

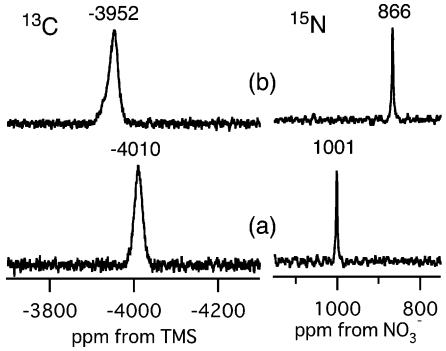

Figure 4. ^{13}C (left) and ^{15}N (right) NMR spectra of the cyanide-1-methylimidazole complex of iron(III) PPDME at 298 K (a) in CD_2Cl_2 and (b) CD_2Cl_2−CD_3OD (22%).

PPDME were located at −4148 and 918 ppm, respectively.[38] In comparison with the ^{13}C and ^{15}N NMR shifts for the 1-methylimidazole complex, both the ^{13}C and ^{15}N NMR signals for the 1,2-dimethylimidazole complex show upfield shifts. This indicates that the tilt of the iron−axial imidazole bond increases the paramagnetic shift of the ^{13}C NMR signal but decreases that of the ^{15}N NMR signal.

To study the effect of solvent on the ^{13}C and ^{15}N NMR shifts of the iron-bound cyanide, ^{13}C and ^{15}N NMR spectra of the iron-bound cyanide were collected in various solvents. The observed ^{13}C and ^{15}N NMR shifts are summarized in Table 1. The ^{13}C and ^{15}N NMR signals of the iron-bound cyanide of iron(III) PPDME with 1-methylimidazole in CD_2Cl_2 are located at −4010 and 1001 ppm, while those in DMSO-d_6 are −4004 and 1012 ppm, respectively. A drastic change in the NMR shift was not observed between CD_2Cl_2 and DMSO-d_6. On the other hand, the positions of the ^{13}C and ^{15}N NMR signals of iron-bound cyanide change considerably upon addition of a protic solvent, such as methanol or H_2O. It is known that these protic solvents form hydrogen bonds with iron-bound cyanide.[17a,39] As shown in Figure 4, with the addition of methanol-d_4 to CD_2Cl_2, the ^{13}C and ^{15}N NMR signals of the iron-bound cyanide are shifted downfield

(34) The *g* parameters for ARP, HO, and FixL were used for the EPR *g* values obtained for these heme proteins in this study.
(35) Caughey, W. S.; Fujimoto, W. Y.; Johnson, B. P. *Biochemistry* **1966**, *5*, 3830−3843.
(36) Albert, A. In *Physical Methods in Heterocyclic Chemistry*; Katritzky, A. R., Ed.; Academic Press: New York, 1971; Vol. III, pp 1−108.
(37) (a) Scheidt, W. R.; Geiger, D. K.; Lee, Y. J.; Reed, C. A.; Lang, G. *J. Am. Chem. Soc.* **1985**, *107*, 5693−5699. (b) Yoshimura, T.; Ozaki, T. *Bull. Chem. Soc. Jpn.* **1979**, *52*, 2268−2275. (c) Ellison, M. K.; Schulz, C. E.; Scheidt, W. R. *Inorg. Chem.* **2002**, *41*, 2173-2181.
(38) The iron-bound 1,2-dimethylimidazole rotates rapidly on the NMR time scale because the ^{1}H NMR signals of all of four heme methyl signals for the cyanide-1,2-dimethylimidazole complex of iron(III) PPDME are observed in the downfield (18.8, 18.5, 15.7, and 15.3 ppm from TMS in CD_2Cl_2 at 298 K), as in the case of the cyanide-1-methylimidazole complex (15.9, 15.4, 13.0, and 12.8 ppm from TMS in CD_2Cl_2 at 298 K).
(39) Frye, J. S.; La Mar, G. N. *J. Am. Chem. Soc.* **1975**, *97*, 3561−3562.

Table 2. ^{13}C and ^{15}N NMR Chemical Shifts of Iron-Bound Cyanides for Heme Proteins in 0.1 M Potassium Phosphate Buffer/D_2O Solution at 298 K

heme protein	^{13}C NMR shift	^{15}N NMR shift	pH
	myoglobin		
horse heart	−4138	948	7.0
sperm whale	−4145	951	7.0
sperm whale H64A	−4221	1005	7.2
	hemoglobin		
human adult[a]	−4074	975, 1047[b]	7.0
	cytochrome *c*		
horse heart	−3761	856[c]	7.2
bovine heart	−3763	859[c]	7.7
yeast	−3727	886[c]	7.4
	peroxidase		
horseradish	−3612	576	7.0
A. ramosus	−3699	574	7.6
	heme oxygenase		
rat	−3750	818, 797	7.4
rat E29A	−3820	808	7.4
P. aeruginosa	−3829	853	7.4
	FixL		
S. meliloti	−4128	905[d]	7.3

[a] In 0.1 M Tris-HCl buffer in D_2O. [b] Ref 17a. [c] Ref 18b. [d] Ref 46.

and upfield, respectively. This indicates a decrease in the ^{13}C and ^{15}N paramagnetic shifts of the iron-bound cyanide as the result of hydrogen-bond formation with the solvent. Similar changes are observed when water is added to DMSO-d_6 (Table 1). Since a hydrogen bond from a solvent induces a more pronounced shift in the ^{15}N NMR signal rather than the ^{13}C NMR signal, the ^{15}N NMR shift of the iron-bound cyanide is much more sensitive to the presence of hydrogen bonds than the ^{13}C NMR shift.

^{13}C and ^{15}N NMR Spectra for Heme Proteins. To study the applicability of the ^{13}C and ^{15}N NMR spectroscopy of the iron-bound cyanide as a NMR probe, we obtained ^{13}C and ^{15}N NMR spectra of the cyanide forms of various ferric heme proteins with a proximal hisitdine. The ^{13}C and ^{15}N NMR shifts of iron-bound cyanide for the various heme proteins are summarized in Table 2. The isotropic shifts, dipolar shifts, contact shifts, and isotropic hyperfine coupling constants, calculated according to eqs 1−4, are summarized in Tables 3 and 4.

The ^{13}C NMR signals of the iron-bound cyanides of whale-Mb and horse-Mb are located at −4138 and −4145 ppm from TMS, respectively. When their broad signals are taken into account, these ^{13}C NMR shifts are almost identical within experimental error. No significant change in the ^{13}C NMR resonance position was found for myoglobin from various origins. In previous studies, the ^{15}N NMR signals of iron-bound cyanide for whale-Mb was observed at +945 ppm, and the resonance position was unchanged in myoglobin from various origins.[17a] To investigate the effect of the distal histidine on the ^{13}C and ^{15}N NMR shifts, we obtained ^{13}C and ^{15}N NMR spectra of iron-bound cyanide for the whale-Mb H64A mutant, in which histidine-64 (the distal hisitidine) is replaced by alanine (Figure 5). The ^{13}C and ^{15}N NMR signals for the whale-Mb H64A mutant were observed at −4221 ppm and +1005 ppm, respectively. With a mutation in the distal histidine, the ^{13}C NMR signal showed an 83 ppm upfield shift, while the ^{15}N NMR signal showed a 60 ppm dowfield shift.

As we reported in a previous communication, the ^{13}C NMR signal of the iron-bound cyanide of human hemoglobin was detected at −4074 ppm from TMS.[21] Although the α and β subunits of human hemoglobin showed different ^{15}N NMR shifts for the iron-bound cyanide, +975 (α) and +1047 (β) ppm,[17a] the ^{13}C NMR signal of the α and β subunits of human hemoglobin were not completely separated.

We also obtained ^{13}C and ^{15}N NMR spectra for iron-bound cyanide in various kinds of cytchrome c. The ^{13}C NMR signals of ferric cyanide complexes of horse-Cyt c, bovine-Cyt c, and yeast-Cyt c were observed at −3761, −3763, and

Table 3. Isotropic, Dipolar, and Contact Shifts of ^{13}C and ^{15}N NMR Signals of Iron-Bound Cyanide for Iron(III) Porphyrin Complexes at 298 K

	^{13}C				^{15}N				
model complex	isotropic shift	dipolar shift[a]	contact shift	A_{iso}	isotropic shift	dipolar shift[a]	contact shift	A_{iso}	$\lvert^{15}N/^{13}C\rvert$
PPDMEFe(1-Me-Im)CN	−4187	+401	−4588	−43.4	+1112	+108	+1002	+3.8	0.218
PPDMEFe(1-Ph-Im)CN	−4243	+401	−4644	−43.9	+1137	+108	+1027	+3.9	0.221
PPDMEFe(1-Ac−Im)CN	−4316	+401	−4717	−44.6	+1109	+108	+1001	+3.8	0.212
PPDMEFe(1,2-DiMe-Im)CN	−4325	+401	−4726	−44.7	+1029	+108	+921	+3.5	0.195
PPDMEFe(ImH)CN	−4103	+401	−4504	−42.6	+1126	+108	+1018	+3.8	0.226
PPDMEFe(Im^-)CN	−3684	+262	−3946	−37.3	+844	+71	+773	+2.9	0.196
DAPDMEFe(1-Me-Im)CN	−4174	+401	−4575	−43.2	+1138	+108	+1030	+3.9	0.225
MPDMEFe(1-Me-Im)CN	−4204	+401	−4605	−43.5	+1106	+108	+998	+3.7	0.217
DPDMEFe(1-Me-Im)CN	−4222	+401	−4623	−43.7	+1125	+108	+1017	+3.8	0.220
PPFe(1-Me-Im)CN	−4178	+401	−4579	−43.3	+1121	+108	+1013	+3.8	0.221
PPFe(ImH)CN	−4144	+401	−4545	−42.9	+1121	+108	+1013	+3.8	0.223
PPFe(DMAP)CN	−4145	+401	−4546	−43.0	+1095	+108	+987	+3.7	0.217
PPFe(4-Me-Py)CN	−4298	+401	−4699	−44.4	+1166	+108	+1058	+4.0	0.225
PPFe(Py)CN	−4335	+401	−4736	−45.1	+1169	+108	+1061	+4.0	0.224
PPFe(4-Ac−Py)CN	−4372	+401	−4773	−45.1	+1166	+108	+1058	+4.0	0.222
PPFe(4-CN−Py)CN	−4446	+401	−4847	−45.8	+1263	+108	+1155	+4.4	0.238
PPDMEFe(1-Me-Im)CN[b]	−4129	+401	−4530	−42.8	+977	+108	+869	+3.3	0.192
PPFe(1-Me-Im)CN[c]	−4111	+401	−4512	−42.6	+1015	+108	+907	+3.4	0.201
PPFe(1-Me-Im)CN[d]	−4052	+401	−4453	−42.1	+941	+108	+833	+3.1	0.187

[a] For the calculations of dipolar shifts,[11c] $g_1 = 3.4$, $g_2 = 1.89$, $g_3 = 0.74$, $r_{Fe-C} = 2.02$ Å, $r_{Fe-N} = 3.12$ Å, and $\theta = 0$ were used for all compounds except the imidazolate complex,[27a] for which $g_1 = 3.1$, $g_2 = 2.2$, $g_3 = 1.4$, $r_{Fe-C} = 2.02$ Å, $r_{Fe-N} = 3.12$ Å, and $\theta = 0$ were used. [b] In CD_2Cl_2−CD_3OD (22%). [c] In DMSO-d_6−H_2O (30%). [d] In DMSO-d_6−H_2O (50%).

Table 4. Isotropic, Dipolar, and Contact Shifts of ^{13}C and ^{15}N NMR Signals for Heme Proteins at 298 K

	^{13}C				^{15}N				
heme protein	isotropic shift	dipolar shift[a]	contact shift	A_{iso}	isotropic shift	dipolar shift[a])	contact shift	A_{iso}	$\lvert^{15}N/^{13}C\rvert$
whale-Mb	−4315	+409	−4724	−44.6	+1059	+117	+942	+3.6	0.199
horse-Mb	−4322	+409	−4731	−44.7	+1062	+117	+945	+3.6	0.200
whale-Mb H64A	−4398	+409	−4807	−45.4	+1116	+117	+999	+3.8	0.208
human-Hb	−4251	+371	−4622	−43.7	+1086 (α)	+106	+980	+3.7	0.212
					+1158 (β)	+100	+1058	+4.0	0.229
horse-Cyt c	−3938	+421	−4359	−41.2	+967	+113	+854	+3.3	0.196
bovin-Cyt c	−3940	+421	−4361	−41.2	+970	+113	+857	+3.3	0.197
yeast-Cyt c	−3904	+421	−4325	−40.9	+997	+113	+884	+3.4	0.204
HRP	−3789	+282	−4071	−38.5	+687	+74	+613	+2.3	0.151
ARP	−3876	+305	−4181	−39.5	+685	+80	+605	+2.3	0.145
rat-HO-1	−3927	+330	−4257	−40.2	+908	+94	+814	+3.1	0.191
rat-HO-1 E29A	−3997	+330	−4327	−40.9	+919	+94	+825	+3.1	0.191
PigA-HO	−4006	+330	−4336	−41.0	+964	+94	+870	+3.3	0.201
Fix-L	−4305	+428	−4733	−44.7	+1016	+121	+895	+3.4	0.189

[a] Dipolar shifts were calculated by using following parameters: Mb[30,47] $g_1 = 3.45$, $g_2 = 1.89$, $g_3 = 0.93$, $r_{Fe-C} = 2.02$ Å, $r_{Fe-N} = 3.06$ Å, $\theta_C = 0$, $\theta_N = 4.8°$; Hb[31,48] $g_1 = 3.41$, $g_2 = 1.88$, $g_3 = 0.75$ (α $r_{Fe-C} = 2.08$ Å, $r_{Fe-N} = 3.13$ Å, $\theta_C = 0$, $\theta_N = 11.4°$; β $r_{Fe-C} = 2.08$ Å, $r_{Fe-N} = 3.21$ Å, $\theta_C = 0$, $\theta_N = 6.5°$); Cyt c[32,49] $g_1 = 3.45$, $g_2 = 1.89$, $g_3 = 0.93$, $r_{Fe-C} = 2.0$ Å, $r_{Fe-N} = 3.1$ Å, $\theta_C = 0$, $\theta_N = 1.2°$; HRP[33,52] $g_1 = 3.05$, $g_2 = 2.1$, $g_3 = 1.2$, $r_{Fe-C} = 1.99$ Å, $r_{Fe-N} = 3.09$ Å, $\theta_C = 0$, $\theta_N = 7.8°$; ARP[34,51] $g_1 = 3.09$, $g_2 = 2.13$, $g_3 = 1.17$, $r_{Fe-C} = 1.96$ Å, $r_{Fe-N} = 3.04$ Å, $\theta_C = 0$, $\theta_N = 8.6°$; HO[34,50] $g_1 = 3.32$, $g_2 = 2.06$, $g_3 = 1.0$, $r_{Fe-C} = 2.07$ Å, $r_{Fe-N} = 3.14$ Å, $\theta_C = 0$, $\theta_N = 4.9°$; FixL[34,53] $g_1 = 3.45$, $g_2 = 1.9$, $g_3 = 1.0$, $r_{Fe-C} = 1.99$ Å, $r_{Fe-N} = 3.03$ Å, $\theta_C = 0$, $\theta_N = 1.8°$.

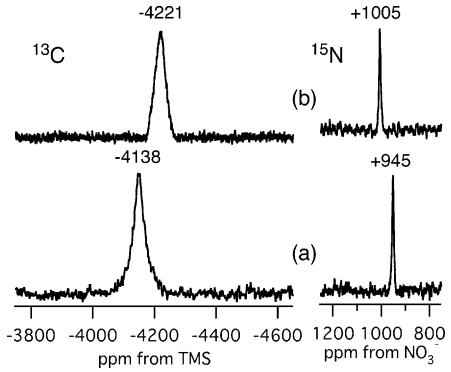

Figure 5. ^{13}C (left) and ^{15}N (right) NMR spectra of the cyanide forms of (a) whale-Mb and (b) whale-Mb H64A in a 0.1 M potassium phosphate buffer/D_2O solution at 298 K.

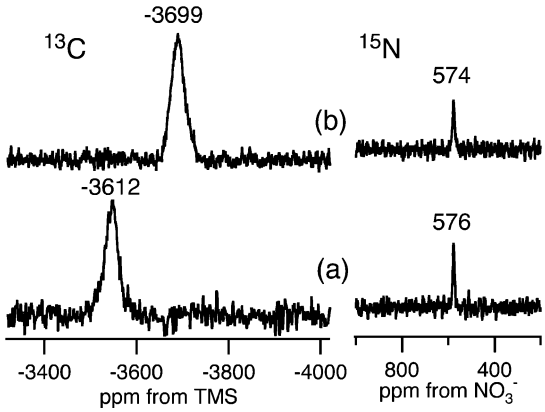

Figure 6. ^{13}C (left) and ^{15}N (right) NMR spectra of the cyanide forms of (a) HRP and (b) ARP in a 0.1 M potassium phosphate buffer/D_2O solution at 298 K.

−3727 ppm, respectively. The ^{15}N NMR spectra of the iron-bound cyanides for these cytochrome *c* were located around ∼860 ppm.[18b] As was the case for myoglobin, the ^{13}C and ^{15}N NMR signals for the ferric cyanide forms of cytochromes c show little species variation.

The ^{13}C NMR shifts of iron-bound cyanides for peroxidases were much smaller than those for myoglobin and cytochrome *c*. Figure 6 shows the ^{13}C NMR signals for the iron-bound cyanide of ferric cyanide complexes of HRP and ARP. The ^{13}C NMR signals for HRP and ARP are located at −3612 and −3699 ppm, respectively. The ^{15}N NMR shifts of iron-bound cyanide for HRP and ARP were detected at 576 and 574 ppm, respectively.[18a,40] In contrast to myoglobin and cytchrome c, the ^{13}C NMR signals varied depending on the origin of the peroxidase, but the^{15}N NMR signal did not.

To apply ^{13}C and ^{15}N NMR spectroscopy to other heme proteins with a proximal histidine, we obtained ^{13}C and ^{15}N NMR spectra for the cyanide forms of heme oxygenase (HO), which catalyzes the degradation of heme to biliverdin.[41]

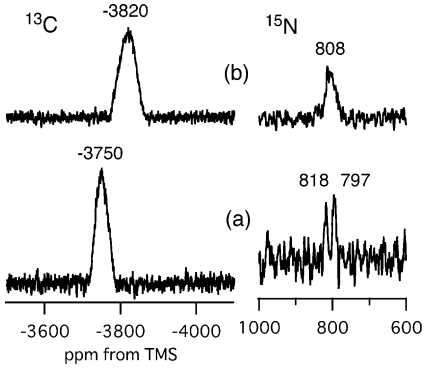

Figure 7. ^{13}C (left) and ^{15}N (right) NMR spectra of cyanide forms of (a) rat-HO and (b) rat-HO E29A mutant in a 0.1 M potassium phosphate buffer/D_2O solution at 298 K.

Figure 7 shows the ^{13}C and ^{15}N NMR spectra of cyanide complexes of rat-HO-1 and its E29A mutant. The ^{13}C NMR signal of rat-HO-1 is located at −3750 ppm. Interestingly, rat-HO-1 shows two ^{15}N NMR signals at 797 and 818 ppm,

(40) Lukat, G. S.; Rodgers, K. R.; Jabro, M. N.; Goff, H. M. *Biochemistry* **1989**, *28*, 3338−3345.

(41) (a) Yoshida, T.; Kikuchi, G. *J. Biol. Chem.* **1978**, *253*, 4224−4229. (b) Yoshida, T.; Kikuchi, G. *J. Biol. Chem.* **1979**, *254*, 4487−4491.

suggesting presence of two cyanide-bound structures. These may be formed from the orientational disorder of heme, the digestion of C-terminal amino acids to 28 kDa, or the conformers that differ in the position of the distal helix.[41b,42] In a crystal structure of rat-HO-1, the NH moiety of the proximal histidine seems to be involved in a hydrogen-bonding interaction with glutamate-29, similar to a peroxidase.[42] To examine the hydrogen-bonding interaction of glutamate-29, we obtained ^{13}C and ^{15}N NMR spectra of the cyanide form of the rat-HO-1 E29A mutant, in which glutamate-29 is replaced with alanine. With the mutation, the ^{13}C NMR signal of the iron bound cyanide shows large upfield shift, but the resonance position of the ^{15}N NMR signal changes only negligibly. We also obtained ^{13}C and ^{15}N NMR spectra of the cyanide form of heme oxygenase from *P. aeruginosa* (PigA-HO).[43] The ^{13}C and ^{15}N NMR signals for PigA-HO were located at -3829 and $+853$ ppm, respectively. These ^{13}C and ^{15}N NMR resonance positions for Pig-HO are slightly larger than those for rat-HO-1.

Hyperfine Coupling Tensors in Heme Proteins. A previous ^{13}C ENDOR study reported on the parallel component, A_z, of the hyperfine coupling constants of the iron-bound cyanide for sperm whale myoglobin and human hemoglobin to be -28.64 and -27.33 MHz, respectively.[44] Therefore, the present isotropic hyperfine coupling constants for the iron-bound cyanides allow their anisotropic hyperfine coupling constants to be determined. The hyperfine coupling constant (A) can be divided into two terms: an isotropic hyperfine coupling constant (A_{iso}) and a dipolar hyperfine coupling constant ($A_{dipolar}$), $A = A_{iso} + A_{diploar}$, and the dipolar hyperfine coupling constant can be treated as a tensor (A_{xx}, A_{yy}, A_{zz}, $A_{xx} + A_{yy} + A_{zz} = 0$). From the present ^{13}C isotropic hyperfine coupling constants for Mb ($A_{iso} = -44.6$ MHz) and Hb ($A_{iso} = -43.7$ MHz), we estimate that the ^{13}C dipolar hyperfine coupling tensor of the iron-bound cyanide for Mb and Hb would be ($A_{xx} = -8.0$ MHz, $A_{yy} = -8.0$ MHz, $A_{zz} = +16.0$ MHz) and ($A_{xx} = -8.2$ MHz, $A_{yy} = -8.2$ MHz, $A_{zz} = +16.4$ MHz), respectively.[45] On the other hand, the ^{15}N ENDOR study also showed the parallel component, A_z, of the hyperfine coupling constant for iron-bound cyanide for sperm whale myoglobin to be $+5.25$ MHz.[44] Since the ^{15}N isotropic hyperfine coupling constant is calculated to be $+3.6$ MHz, the ^{15}N dipolar hyperfine coupling tensor would be ($A_{xx} = -0.85$ MHz, $A_{yy} = -0.85$ MHz, $A_{zz} = +1.7$ MHz).[45]

Discussion

Paramagnetic Shift of Iron-Bound Cyanide. The ^{13}C and ^{15}N NMR signals of iron-bound cyanides of ferric heme proteins and related model complexes are located in the far upfield and downfield regions, respectively. For all heme proteins and their model complexes, the contributions of the dipolar shift for the ^{13}C and ^{15}N signals of the iron-bound cyanides are much smaller than those of the contact shifts: $+200$ to $+400$ ppm for ^{13}C NMR and $+50$ to $+130$ ppm for ^{15}N NMR. Thus, the extremely large paramagnetic shifts of the ^{13}C and ^{15}N NMR signals of the iron-bound cyanide result from contact shifts (see Tables 3 and 4). Interestingly, the contact shifts of the ^{13}C NMR signals of the iron-bound cyanides are negative, but those for the ^{15}N NMR signals are positive. These findings can be explained by the spin-polarization mechanism from the ferric low-spin iron center, as shown in Scheme 2. The unpaired electron of the ferric low spin iron is mainly occupied in the dπ (d_{xz} or d_{yz}) orbital. This electron spin induces a positive spin in the σ-bonding orbitals, such as d_{z^2} or 3s orbitals. The induced spin polarizes a negative spin on the carbon atom of the iron-bound cyanide, and the negative spin on the carbon atom then polarizes a positive spin on the nitrogen atom of the iron-bound cyanide. The negative spin on the carbon atom of the iron-bound cyanide induces a large upfield shift of its ^{13}C NMR signal, while the positive spin on the nitrogen atom induces a large downfield shift of its ^{15}N NMR signal.

Scheme 2

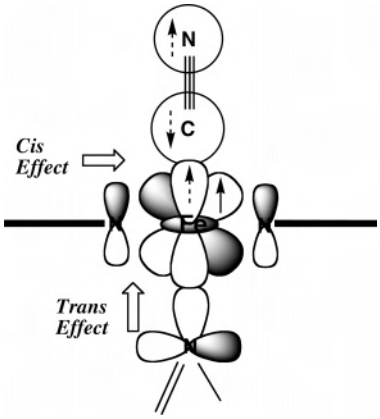

^{13}C and ^{15}N NMR Shifts of Iron-Bound Cyanide of Ferric Heme Complexes. The ^{13}C and ^{15}N NMR spectra of the iron-bound cyanides of iron(III) porphyrin complexes presented here clearly show that both the ^{13}C and ^{15}N NMR shifts of the iron-bound cyanide are not very sensitive to the electronic effects originating from the porphyrin ring. Therefore, the various heme structures that are known to be present in natural heme proteins would not significantly affect their NMR shifts, and the iron-bound cyanide is suitable as an NMR probe for studying proximal and distal environments in a heme protein

The ^{13}C and ^{15}N NMR resonance positions are very sensitive to an electronic effect from the proximal ligand. The ^{13}C NMR signal is a very sensitive tool for monitoring donor effects from the proximal ligand. As the donor effect of the proximal imidazole increases, the paramagnetic shift of the ^{13}C NMR signal of the iron-bound cyanide is decreased. This can be explained by the trans ligand effect of the proximal imidazole (Scheme 2). As the donor effect of the proximal imidazole is increased, the binding of cyanide coordinated at the opposite position of the proximal imidazole

(42) Schuller, D. J.; Wilks, A.; Oritz de Montellano, P. R.; Poulos, T. L. *Nat. Struct. Biol.* **1999**, *6*, 860−867.
(43) Ratliff, M.; Zhu, W.; Deshmukh, R.; Wilks, A.; Stojiljkovic, I. *J. Bacteriol.* **2001**, *183*, 6394−6403.
(44) Mulks, C. F.; Scholes, C. P.; Dickinson, L. C.; Lapidot, A. *J. Am. Chem. Soc.* **1979**, *101*, 1645−1654.
(45) Dipolar hyperfine coupling tensors for ^{13}C and ^{15}N atoms of the iron bound cyanide were assumed to have an axial symmetry: $A_{xx} = A_{yy}$.

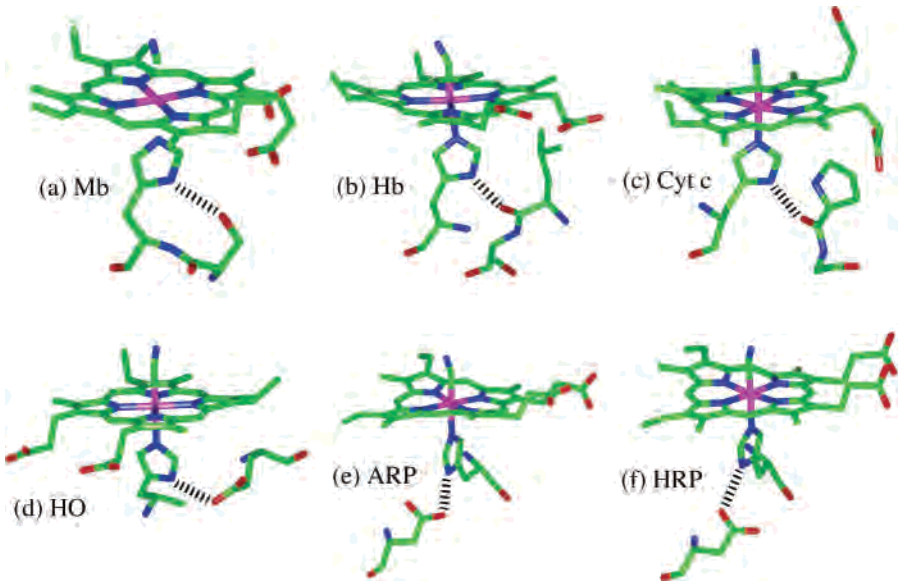

Figure 8. Hydrogen-bonding interactions of proximal histidines with various proton acceptors in heme proteins:[47−52] (a) whale-Mb, (Protein Data Bank (PDB) 1EBC) (b) human-Hb (PDB 1ABY), (c) horse cyt c (PDB 1FHB), (d) rat-HO (PDB 1IX3), (e) ARP (PDB 1ARU), and (f) HRP (PDB 7ATJ).

becomes weak as a result of the trans ligand effect. Thus, the spin density on the ^{13}C atom polarized by the ferric iron center would be smaller with an increase in the donor effect, resulting in a small paramagnetic shift in the ^{13}C NMR signal of the iron-bound cyanide. As shown in Figure 2 and Figure S1, the ^{15}N NMR shift of the iron-bound cyanide is less sensitive than the ^{13}C NMR shift to the trans ligand effect. Since the electron spin on the^{15}N atom is polarized via the electron spin on the^{13}C atom, the effect of a trans ligand on the ^{15}N NMR shift is not drastic.

For the hydrogen-bonding effect from the solvent, the ^{15}N NMR shift of the iron-bound cyanide is more sensitive than the ^{13}C NMR shift. A drastic decrease in the ^{15}N paramagnetic shifts of the iron-bound cyanide was observed because solvent protons interact with the ^{15}N atom of the iron-bound cyanide.[17a,39] The hydrogen-bonding interaction to the ^{15}N atom decreases the spin density at the ^{15}N atom of cyanide rather than the ^{13}C atom, leading to a small paramagnetic shift of the ^{15}N NMR signal. However, it should be emphasized here that the observed ^{15}N NMR shift for the iron-bound cyanide reflects both the donor effect of the proximal ligand and the hydrogen-bonding effects of the distal side. Therefore, distal hydrogen-bonding interactions in heme proteins are difficult to detect from the ^{15}N NMR shift alone. To evaluate nature of the hydrogen-bonding interactions, the ratio of ^{13}C and ^{15}N NMR contact shifts for the iron-bound cyanide would be a useful parameter, and this is discussed in detail in the next section.

A previous ^{15}N NMR study reported that the ^{15}N NMR shift of the iron-bound cyanide increased with an increase in the pK_a value of the proximal pyridine ligand.[17a] However, the result shown in Figure 2 indicates a decrease in the ^{15}N NMR shift with an increase in the pK_a value of the proximal pyridine ligand. Although the authors explained their result with the trans effect of the proximal ligand, the trans effect should result in a decrease in the ^{15}N NMR shift of the iron-bound cyanide with an increase in the donor effect of the proximal ligand, as discussed above. It is likely that the previous ^{15}N NMR data reflect the hydrogen-bonding effect from solvent water rather than the donor effect of a proximal ligand. With an increase in the pK_a value of pyridine, water molecules in the NMR solvent would form hydrogen bonds more predominantly with pyridine than with the iron-bound cyanide. Therefore, with an increase in the pK_a value of pyridine, the hydrogen-bonding effect from water to the iron-bound cyanide become weaker, leading to an increase of the ^{15}N NMR shift as observed in the previous study. In fact, while we collected the ^{15}N NMR spectra in DMSO-d_6, the previous ^{15}N NMR measurements were done in a pyridine−water mixture.

^{13}C and ^{15}N NMR Signals of Iron-Bound Cyanide in Heme Proteins. As shown in Table 2, the paramagnetic shift of the ^{13}C NMR signals of the iron-bound cyanide of the ferric heme proteins are observed to cover a wide range. The paramagnetic shift increases in the following order: HRP < ARP < HO ≈ Cyt c < Hb < FixL ≈ Mb.[46] The order of the paramagnetic shifts for heme proteins can be explained primarily by the hydrogen-bonding interactions of the proximal histidine and secondarily by the orientation of proximal imidazole plane to the heme.

Figure 8 shows structures of the active site of these heme proteins.[47−52] In these heme proteins, the imidazole NH

(46) Tanaka, A.; Nakamura, H.; Shiro, Y.; Fujii, H. *Biochemistry* **2006**, *45*, 2515−2523.
(47) Bolognesi, M.; Rosano, C.; Losso, R.; Borassi, A.; Rizzi, M.; Wittenberg, J. B.; Boffi, A.; Ascenzi, P. *Biophys. J.* **1999**, *77*, 1093−1099.
(48) Looker, D.; Abbott-Brown, D.; Cozart, P.; Durfee, S.; Hoffman, S.; Mathews, A. J.; Miller-Roehrich, J.; Shoemaker, S.; Trimble, S.; Fermi, G.; Fermi, G.; Komiyama, N. H.; Nagai, K.; Stetler, G. L. *Nature* **1992**, *356*, 258−260.
(49) Banci, L.; Bertini, I.; Bren, K. L.; Gray, H. B.; Sompornpisut, P.; Turano, P. *Biochemistry* **1995**, *34*, 11385−11398.
(50) Sugishima, M.; Sakamoto, H.; Noguchi, M.; Fukuyama, K. *Biochemistry* **2003**, *42*, 9898−9905.
(51) Fukuyama, K.; Kunishima, N.; Amada, F.; Kubota, T.; Matsubara, H. *J. Biol. Chem.* **1995**, *270*, 21884−21892.

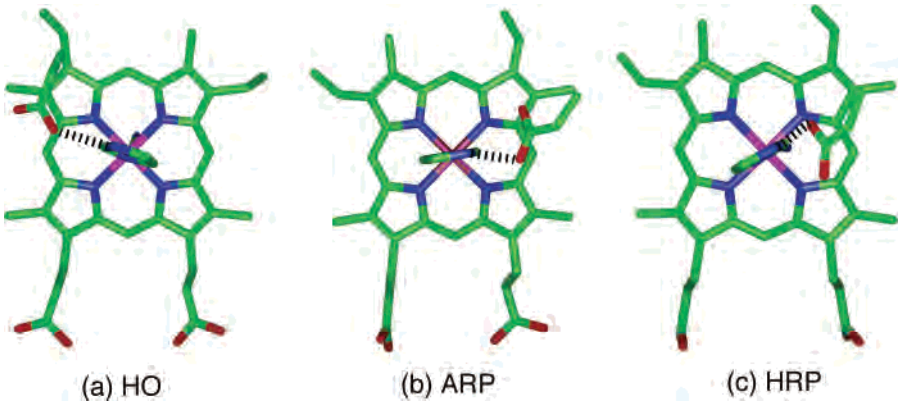

Figure 9. Orientation of the proximal imidazole plane in various heme proteins:[50−52] (a) rat-HO (PDB 1IX3), (b) ARP (PDB 1ARU) (c) HRP (PDB 7ATJ).

moieties of the proximal ligands enter into hydrogen-bonding interactions with a variety of proton acceptors. In HRP, ARP, and HO, the proximal imidazole NH protons form hydrogen bonds with aspartate or glutamate residue.[42,50−52] The aspartate or glutamate residue aggressively deprotonates the proximal imidazole NH proton and shifts the character of the proximal imidazole to an imidazolate, which increases the donor effect from the proximal ligand to the heme iron. Therefore, as shown in the model complexes, the paramagnetic shifts of the ^{13}C NMR signals for HRP, ARP, and HO are smaller than those for the other heme proteins. In fact, the ^{13}C NMR shift for HRP is very close to that of the imidazolate model complex. On the other hand, the proximal histidines of Cyt c and Hb form hydrogen bonds with the carbonyl oxygen of the main chain. These proton acceptors for Cyt c and Hb do not deprotonate the proximal histidine NH proton strongly.[48,49] Thus, the donor effect of the proximal ligands in Cyt c and Hb are weaker than those in peroxidases. As a result, the paramagnetic shifts of the ^{13}C NMR signals for Cyt c and Hb are larger than those of peroxidases. Since the ^{13}C NMR shift for Hb is much larger than that for Cyt c, the hydrogen-bonding interactions for Hb are weaker than those for Cyt c. In Mb and FixL, a serine residue and a water molecule interact with the NH protons of the proximal ligands, respectively.[47,53] Since the serine residue and a water do not extensively deprotonate the NH proton, the ^{13}C paramagnetic shifts for the iron bound cyanide of Mb and FixL are the largest of these heme proteins.[46] In fact, the ^{13}C NMR shifts for Mb and FixL are close to those of the iron(III) porphyrin model complexes.

While the proximal histidines of HRP, ARP, and HO have interactions with a carboxylate residue, the ^{13}C NMR signals of the iron-bound cyanides for these heme proteins are located at different positions. The ^{13}C NMR signals for HRP and ARP show quite different NMR shifts of more than 100 ppm. These changes can be explained by the orientation of the proximal imidazole plane. As shown in Figure 9, the proximal imidazole plane of HRP is parallel to the N−N axis, while those in ARP and HO adopt a staggered conformation relative to the N−N axis. The parallel orientation can overlap the π orbital of the iron-bound N atom of the proximal imidzaole with the iron dπ orbital, but the staggered orientation cannot (Scheme 2). Therefore, the donor effect of the proximal histidine in HRP is transferred to the heme iron more effectively than those in ARP and HO. This results in larger ^{13}C NMR shifts for ARP and HO than that for HRP. Furthermore, as shown in Figure 9, it should be considered that the hydrogen-bonding interaction of the aspartate or glutamate to the proximal histidine is different among these proteins. Indeed, the aspartate or glutamate residue interacting with the proximal histidine has different orientations in these three proteins, and the hydrogen bond distance between the proximal histidine and the aspartate or glutamate residue is also different: (HO) 2.81, (ARP) 2.92, and (HRP) 2.86 Å.[50−52] The difference in the hydrogen-bond distance between ARP and HRP may also explain the order of their ^{13}C NMR shifts. Although the hydrogen-bond distance in HO is the shortest in these heme proteins, the ^{13}C NMR shift for HO is the largest. Since the glutamate residue in HO is in a suitable position to accept the histidine NH proton (see Figure 9a), the imidazolate nature of the proximal histidine in HO is weaker than those in ARP and HRP. The weak imidazolate character, as well as the staggered conformation in HO, would weaken the donor effect of the proximal imidazole, resulting in the largest upfield shift of the ^{13}C NMR signal of the iron bound cyanide in these proteins. The hydrogen-bonding interaction of the proximal histidine would also explain the order of the ^{13}C NMR shifts between Cyt c and Hb. Indeed, the hydrogen bond distance (2.78 Å) between the proximal histidine and the carbonyl oxygen in Cyt c is much shorter than that (av 2.97 Å) of Hb.[48,49] As summarized in Table 2, we measured ^{13}C NMR spectra for Mb and Cyt c from various species but did not see significant change between whale- and horse-Mb or among the horse-, bovine-, and yeast-Cyt c. This is because the hydrogen-bonding interaction and orientation of the proximal imidazole are not significantly changed by the origin of Mb or Cyt c.[47,54,55]

(52) Henriksen, A.; Smith, A. T.; Gajhede, M. *J. Biol. Chem.* **1999**, *274*, 35005−35011.

(53) (a) Hao, B.; Isaza, C.; Arndt, J.; Soltis, M.; Chan, M. K. *Biochemistry* **2002**, *41*, 12952−12958. (b) Miyatake, H.; Mukai, M.; Park, S.-Y.; Adachi, S.; Tamura, K.; Nakamura, H.; Nakamura, K.; Tsuchiya, T.; Iizuka, T.; Shiro, Y. *J. Mol. Biol.* **2000**, *301*, 415−431.

(54) Bisig, D. A.; Iorio, E. E.; Diederichs, K.; Winterhalter, K. H.; Piontek, K. *J. Biol. Chem.* **1995**, *270*, 20754−20762.

The donor effect of the proximal histidine on the ^{13}C NMR shift of the iron-bound cyanide is further confirmed by good correlations of the ^{13}C NMR shift with the ^{1}H NMR shift of the proximal imidazole NH proton of a ferric cyanide form and with the stretching frequency of the iron−axial imidazole bond of a ferrous deoxy form obtained from resonance Raman spectroscopy (see Figure S2 and S3). Previous studies have shown that the ^{1}H NMR shift of the proximal imidazole NH proton and the stretching frequency of the iron−axial imidazole bond reflect the strength of the iron−axial imidazole bond.[56,57] The correlations of the ^{13}C NMR shift of the iron-bound cyanide with these data support that the ^{13}C NMR signal of the iron-bound cyanide is a sensitive probe to estimate the nature of the proximal histidine ligand.

As another minor effect, we need to take into account the tilt of the iron−axial imidazole bond. The present model study showed the tilt of the iron−axial imidazole bond increases in the paramagnetic shift (138 ppm) of ^{13}C NMR signal of the iron-bound cyanide and decreases that (82 ppm) of the ^{15}N NMR signal (see Figure 3). Furthermore, the bent and tilt angles of the iron-bound cyanide may also affect the ^{13}C and ^{15}N NMR shifts of the iron bound cyanide; however, the effects would not be so drastic. This is supported by the ^{13}C and ^{15}N NMR shifts of whale-Mb and horse-Mb being almost identical, despite having different bent angles in their X-ray crystal structures: 166° for whale-Mb and 137° for horse-Mb.[47,54]

The ^{13}C and ^{15}N NMR paramagnetic shifts of the iron-bound cyanide are induced by the electron spin of the heme iron. Since the electron spin on the N atom of the iron-bound cyanide is polarized via the C atom of the cyanide, the ^{15}N NMR paramagnetic shift of the iron-bound cyanide would correlate with its ^{13}C paramagentic NMR shift. To determine the correlation between the ^{13}C and ^{15}N NMR shifts for the iron-bound cyanide, we calculated the ratio of the ^{13}C and ^{15}N NMR contact shifts, $|^{15}N$ NMR shift/^{13}C NMR shift|, for the iron-bound cyanide for iron(III) porphyrin complexes and heme proteins (see Figure S4 and Tables 3 and 4). The ratios for the iron(III) porpyhrin model complexes were calculated to be ∼0.22. A similar value would be expected for the heme proteins if there were no interactions with the iron bound cyanide. However, the ratios for the heme proteins were smaller than the values for the model complexes. This is caused by the hydrogen-bonding interactions in distal proton donors in the heme proteins. As shown in this study, the ^{15}N NMR shift is decreased more drastically by distal hydrogen-bonding interactions than the ^{13}C NMR shift. Therefore, the ratio is decreased with an increase in such interactions. In fact, the ratios for the model complexes are decreased when water or methanol is added to the solvent.

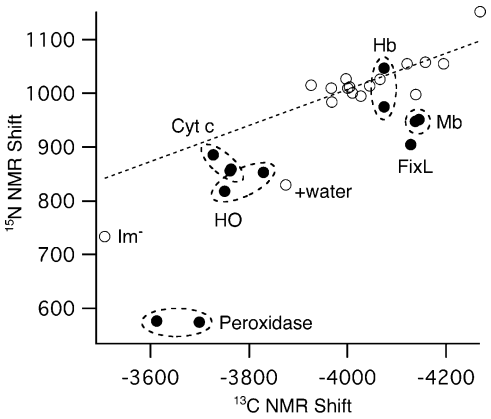

Figure 10. Correlation of ^{13}C and ^{15}N NMR shifts. Filled and open circles show NMR shifts for heme proteins and model complexes, respectively. The broken line shows the correlation line for the model complexes.

Furthermore, this is also confirmed by the increase in the ratio for the whale-Mb H64A mutant, in which a hydrogen-bonding interaction from the distal histidine residue is absent. In peroxidases, it is known that the well-conserved histidine and arginine residues interact strongly with the iron-bound cyanide N atoms.[51,52] Furthermore, the arginine residue and a water molecule interact with the N atoms of the iron-bound cyanides in the crystal structures of FixL and rat-HO-1, respectively.[50,53a] As a result, these hydrogen-bonding interactions would decrease the ratios for these heme proteins. The ratio of the ^{13}C and ^{15}N NMR shifts would be a useful parameter for detecting distal hydrogen-bonding interactions in a heme protein with the proximal histidine.

Finally, to visualize the effects of proximal and distal hydrogen bonding in the heme proteins discussed here, a $^{13}C/^{15}N$ NMR correlation plot is shown in Figure 10. As discussed above, the ^{15}N NMR shifts for the model complexes in organic solvents are linearly correlated with the ^{13}C NMR shifts. The points for the imidazolate complex and the model complex in an aqueous solvent are away from this line because of the hydrogen-bonding interactions from the protic solvents in the sample solutions. Interestingly, the points for the heme proteins are located in different areas, depending on the function of the protein. Although insufficient points are available to make a firm conclusion, the results suggest that the $^{13}C/^{15}N$ correlation plot could be used to differentiate the protein function and would be useful for estimating the function of unknown proteins with the proximal histidine.

In summary, we report a ^{13}C and ^{15}N NMR study of iron-bound cyanides in heme proteins and related model complexes. The findings show that the application of a combination of ^{13}C and ^{15}N NMR spectroscopy to iron-bound cyanide represents a powerful tool for characterizing the nature of the proximal and distal environments in a heme protein with the proximal histidine. The ^{13}C NMR signal of the iron-bound cyanide is a sensitive probe for estimating the donor effect of the proximal imidazole. Hydrogen-bonding interactions involving the iron-bound small molecule from the distal side can be estimated from the ratio of the ^{13}C and ^{15}N NMR shift of the iron-bound cyanide.

(55) (a) Bushnell, G. W.; Louie, G. V.; Brayer, G. D. *J. Mol. Biol.* **1990**, *214*, 585−595. (b) Berghuis, A. M.; Guillemette, J. G.; McLendon, G.; Sherman, F.; Simth, M.; Brayer, G. D. *J. Mol. Biol.* **1994**, *236*, 786−799.

(56) (a) Nagai, K.; La Mar, G. N.; Jue, T.; Bunn, H. F. *Biochemistry* **1982**, *21*, 842−847. (b) La Mar, G. N.; de Ropp, J. S. *J. Am. Chem. Soc.* **1982**, *104*, 5203−5206. (c) Goff, H. M.; La Mar, G. N. *J. Am.Chem. Soc.* **1977**, *99*, 6599−6606.

(57) Teraoka, J.; Kitagawa, T. *J. Biol. Chem.* **1981**, *256*, 3969−3977.

Acknowledgment. This work was supported by grants from the Ministry of Education, Culture, Sports, Science and Technology, Japan and from the Japan Science and Technology Agency, CREST.

Supporting Information Available: ^{13}C (left) and ^{15}N (right) NMR spectra of cyanide complexes of iron(III) PPDME with various imidazole axial ligands (Figure S1), plots of the ^{1}H NMR shift of the proximal imidazole NH proton over the ^{13}C NMR shift of the iron-bound cyanide (Figure S2) and over the stretching frequency of the iron−axial imidazole bond of a ferrous deoxy form (Figure S3), and ratios of ^{13}C and ^{15}N NMR contact shifts for heme proteins and related model complexes (Figure S4). This material is available free of charge via the Internet at http://pubs.acs.org.

IC0607383